

# New spectral assignment of n-propanol in the C—H stretching region

Yuanqin Yu,<sup>a</sup> Yuxi Wang,<sup>b</sup> Ke Lin,<sup>b</sup> Xiaoguo Zhou,<sup>b</sup> Shilin Liu<sup>b\*</sup> and Jin Sun<sup>a</sup>



The C—H stretching vibration serves as an important probe for characterizing molecular structures and properties of hydrocarbons. In this work, we present a detailed study on gas-phase Raman spectrum of n-propanol in the C—H stretching region using stimulated photoacoustic Raman spectroscopy. A complete assignment was carried out with the aid of quantum chemistry calculations and depolarization ratio measurement as well as isotope substitutions, i.e. CH<sub>3</sub>CD<sub>2</sub>CD<sub>2</sub>OH, CD<sub>3</sub>CH<sub>2</sub>CD<sub>2</sub>OH and CD<sub>3</sub>CD<sub>2</sub>CH<sub>2</sub>OH. It is shown that the spectra of three C—H groups of n-propanol overlap each other because of Fermi resonance coupling and different molecular conformations, leading to complex features that were not determined previously. In addition, the comparisons between the spectra of three isotopologues reveal that the C—H vibrations at different sites of carbon chain exhibit different sensitivity to conformational change of n-propanol. The CH<sub>3</sub> stretching vibration at terminated  $\gamma$ -carbon is not sensitive whereas the CH<sub>2</sub> stretching vibrations at both  $\alpha$ -carbon and  $\beta$ -carbon atoms are sensitive. Furthermore, Raman spectra of liquid propanol recorded by conventional spontaneous Raman technique are reassigned on the basis of gas-phase analysis. Copyright © 2016 John Wiley & Sons, Ltd.

Additional supporting information may be found in the online version of this article at the publisher's web site.

**Keywords:** C—H stretching region; n-propanol; photoacoustic Raman spectroscopy

## Introduction

The C—H functional groups are ubiquitous in organic and biological molecules. Their stretching vibrations in the region of 2800 and 3100 cm<sup>-1</sup> are widely used as a probe to investigate intermolecular interaction, conformational change, energy transfer mechanism, vapor/liquid interfacial properties and chemical imaging in biological tissues.<sup>[1–8]</sup> This benefits from the features that the C—H stretching mode is highly localized, and it has large intensity in both infrared and Raman measurements. In addition, the C—H stretching vibration is sensitive to structural changes of molecules. However, unlike other probes such as amide bands, O—H stretches, C—O stretches and N—H stretches,<sup>[9–11]</sup> the C—H stretching modes are challenging to assign because of the pervasive presence of stretch–bend Fermi resonance interactions, leading to complicated band shape that is poorly understood. To systematically investigate the influence of Fermi resonance on the shape of C—H stretching spectra, Snyder *et al.* have ever carried out benchmark studies on alkane systems using low-temperature Raman technique and pointed out that the spectra in the region of 2800–2950 cm<sup>-1</sup> arise from Fermi resonance progressions of polymethylene chain in alkanes.<sup>[12–14]</sup> Furthermore, to make explicit assignment for these Fermi resonance bands, Wang group developed a set of the polarization selection rules to distinguish the bands of Fermi resonance pairs from the asymmetric stretching modes of the methyl and methylene groups based on the symmetric analysis and polarization combinations of sum-frequency generation (SFG) vibrational spectrum at interfaces.<sup>[15–18]</sup> In their study, one important conclusion is that many peaks in the 2920–2940 cm<sup>-1</sup> region were incorrectly assigned to the asymmetric modes of methyl and methylene in the literature or databases, but actually they belong to one of the Fermi resonance pairs between the symmetric stretching and bending overtone of methyl

or methylene groups. Their results are widely used for the spectral assignments of methyl or methylene groups, especially in the SFG studies.

It is well known that quantum chemistry calculations generally provide powerful support for the assignment of experimental spectra. However, it is still a challenge to predict an accurate spectrum in the C—H stretching region because of large anharmonic effect and Fermi resonance interaction, which make the comparison between theoretical and experimental spectra difficult. To establish a direct contrast with the observed spectrum, several research groups recently developed theoretical models to simulate spectral details in the C—H stretching region.<sup>[19–26]</sup> For example, Gerber group developed anharmonic vibrational self-consistent field method and the C—H stretching spectra were well reproduced without any scaling for a series of organic molecules, such as long chain hydrocarbons, dodecane.<sup>[20–22]</sup> Based on a local mode Hamiltonian that incorporates cubic stretch–bend coupling, Sibert group recently developed a first-principle model for accurately describing the Fermi resonance coupling in the alkyl C—H stretching region.<sup>[23–26]</sup>

To explicitly assign the congested C—H stretching bands, a highly resolved experimental spectrum is required. In the condensed phase, the vibrational spectra are usually broadened

\* Correspondence to: Shilin Liu, Department of Chemical Physics, University of Science and Technology of China, Hefei 230026, China. E-mail: slliu@ustc.edu.cn

a School of Physics and Material Science, Anhui University, Hefei, Anhui, 230039, China

b Hefei National Laboratory for Physical Sciences at the Microscale, iChEM (Collaborative Innovation Center of Chemistry for Energy Materials), Department of Chemical Physics, University of Science and Technology of China, Hefei 230026, China

because of molecular interactions, such as hydrogen bond. As a result, some important spectral details are buried. A way to achieve high-resolution vibrational spectrum is to switch gas-phase Raman spectroscopy because the gas-phase molecules are almost free from molecular interactions that broaden the spectra in liquid state. More importantly, the gas-phase Raman spectrum exhibits narrow and separated peak shapes because of the fact that Raman selection rules emphasize the sharp Q-branch over the broad rovibrational profiles present in infrared spectrum. As a result, more spectral details are revealed. In recent studies, we have completely assigned the vibrational spectra of some alcohols in the C—H stretching region using gas-phase photoacoustic Raman spectroscopy (PARS).<sup>[27–29]</sup> The results show that the C—H spectra are much more complex than previously determined, even for simple alcohols such as methanol, ethanol and 2-propanol. This brings the confusions in understanding some important dynamical processes based on earlier assignments.<sup>[6,30–32]</sup> In this work, we examine the spectra of another important alcohol molecule, n-propanol, in the C—H stretching region, as part of a program designated to provide reliable spectral groundwork for alcohols and better develop the C—H vibration as a probe of molecular structures. This is an area of research continuing to receive considerable interest.<sup>[16,19,20,24,33]</sup>

N-propanol is usually used as a common solvent in chemical, pharmaceutical and cosmetic industry, also as a model compound in basic biochemical research. It consists of a hydroxyl group (—OH) and an alkyl chain —CH<sub>2</sub>CH<sub>2</sub>CH<sub>2</sub>. The latter is a moiety of many hydrocarbons and biological molecules, such as side chain of amino acid. In previous studies, the vibrational spectrum of n-propanol has been investigated by various methods, including gas-phase and liquid IR spectroscopy, liquid Raman spectroscopy and SFG spectroscopy at gas/liquid interfaces as well as quantum chemistry calculation.<sup>[16,34,35]</sup> However, there is no consistent assignment in the C—H stretching region. It should be especially mentioned that Edwards *et al.* have recently studied Raman spectra of liquid CH<sub>3</sub>CH<sub>2</sub>CH<sub>2</sub>OH in conjunction with its deuterated isotopologues CH<sub>3</sub>CH<sub>2</sub>CD<sub>2</sub>OH, CH<sub>3</sub>CD<sub>2</sub>CH<sub>2</sub>OH and CD<sub>3</sub>CH<sub>2</sub>CH<sub>2</sub>OH, with the aim to give more improved assignment for various C—H stretching bands.<sup>[35]</sup> However, their assignment did not include the Fermi resonance interactions. Additionally, the spectral contributions from different conformations of n-propanol were not considered because n-propanol has five conformers. In our recent work on deuterated n-propanol (CD<sub>3</sub>CH<sub>2</sub>CD<sub>2</sub>OH), it is shown that the stretching vibration of β-CH<sub>2</sub> group is very sensitive to conformational change of n-propanol.<sup>[33]</sup> Therefore, the conformation should play an important role in the determination of the C—H spectra of n-propanol.

N-propanol molecule contains three —CH groups, α-CH<sub>2</sub>, β-CH<sub>2</sub> and γ-CH<sub>3</sub>, respectively, which will result in severe spectral overlapping in the C—H stretching region. Here, we employed the deuterated samples, CH<sub>3</sub>CD<sub>2</sub>CD<sub>2</sub>OH, CD<sub>3</sub>CH<sub>2</sub>CD<sub>2</sub>OH and CD<sub>3</sub>CD<sub>2</sub>CH<sub>2</sub>OH to totally eliminate the spectral interference. Thus, the spectral contribution from each —CH group can be clearly distinguished. On the other hand, the sensitive PARS was used to obtain high-resolution Raman spectrum at very low pressure. In Raman measurement, the depolarization ratio provides the information on symmetric categories of vibrational modes, which serves an important aid for correctly assigning experimental spectra, especially with combining the theoretical calculations. As mentioned early, there are large anharmonic effect and Fermi resonance interaction in the C—H stretching region. Several methods are proposed to addressing anharmonic calculations.<sup>[20–26,36]</sup> Among them, the simplest one is the method of second-order perturbation theory

developed by Barone, a black-box procedure implemented in the GAUSSIAN 09 program.<sup>[36]</sup> However, from a technical point of view, the second-order perturbation theory computations are often plagued by Fermi resonances, especially for large molecular systems.<sup>[37,38]</sup> Therefore, in this study, the calculated harmonic frequencies were scaled by an empirical factor of 0.973 in both C—H bending and stretching regions to guide spectral assignment. Although the theoretical spectra do not agree well with experimental one, it provides reasonable support for the explanations of experimental spectra. Additionally, to provide more information about the impact of intermolecular interaction on the C—H spectra, Raman spectra of liquid n-propanol were recorded with conventional spontaneous Raman technique.

As a molecule with two torsional freedoms, CCCO and CCOH, the conformation of n-propanol has been the subjects of various experimental and theoretical studies.<sup>[10,11,39–42]</sup> So another important objective of this study is to compare the sensitivity of C—H stretching vibration at different sites of carbon backbone chain toward conformational change of n-propanol. Our recent study has shown that symmetric stretching vibration of CH<sub>2</sub> group at β-carbon atom is very sensitive to conformational structures of n-propanol. One question is if the C—H vibrations at another two carbon atoms, α-carbon and γ-carbon atoms, are also sensitive. As a matter of fact, it is of great importance to investigate the sensitivity of site-specific C—H stretching vibration toward molecular conformation because hydrocarbon chains are important structural units in organic and biological molecules.<sup>[43–45]</sup> We hope that the studies on small typical molecule can yield important insight into larger molecules containing —CH groups.

## Experimental and computational methods

Normal n-propanol (CH<sub>3</sub>CH<sub>2</sub>CH<sub>2</sub>OH) is obtained from Sigma-Aldrich (>99.8%, gas chromatography grade). Deuterated n-propanol, CH<sub>3</sub>CD<sub>2</sub>CD<sub>2</sub>OH, CD<sub>3</sub>CH<sub>2</sub>CD<sub>2</sub>OH and CD<sub>3</sub>CD<sub>2</sub>CH<sub>2</sub>OH, was purchased from ICON isotopes, whose purity was checked by gas chromatography and found to be more than 99%.

### Polarized PARS

The basic theory and experimental setup of PARS have been fully described in previous papers,<sup>[27–29,46,47]</sup> but to be complete, only a short description is presented. When the frequency difference between two laser beams (pump and Stokes beams) is resonant with a Raman-active vibrational transition, a stimulated Raman scattering process occurs and the ground-state molecules are transferred to the vibrationally excited state. Then collisions cause the excitation energy to be converted into local heating, which creates a sound wave that is detected by a microphone. The sensitivity of PARS is greatly increased compared to conventional spontaneous Raman measurement, in which the signal from Raman scattering photons is very weak. On the other hand, Raman depolarization ratio can be accurately determined by measuring and fitting the *I*–*θ* curve because PARS intensity (*I*) is periodically dependent on the cross angle (*θ*) between the polarization directions of two laser beams. More straightforwardly, the intensity ratios of *θ* = 90° and *θ* = 0° are the depolarization ratio, where *θ* = 90° and *θ* = 0° mean that the polarization directions of the two laser beams are orthogonal and parallel to each other, respectively. In the present study, the depolarization ratio was obtained by fitting the *I*–*θ* curve because it is more accurate.<sup>[47]</sup>

In experiment, the second-harmonic output of 532.1 nm from a pulsed Nd:YAG laser (line width  $1.0\text{ cm}^{-1}$ , pulse width 10 ns) was split into two beams by a quartz wedge. About 90% of the 532.1-nm laser energy directly entered into the dye laser system (line width  $0.05\text{ cm}^{-1}$ ) for generating a tunable Stokes beam (623–638 nm), and the remainder was used as a pump beam for PARS. The two linearly polarized laser beams were focused in the center of the photoacoustic cell with counterpropagating configuration. The photoacoustic signal is monitored by an oscilloscope to obtain the PARS intensity or averaged by a boxcar integrator to obtain the PARS spectrum. The energies of pump and Stokes beams are typically 10 and 6 mJ/pulse, respectively, and the sample pressure is kept at 5 Torr. The obtained PARS spectrum is normalized to the intensity of Stokes beam, and the wavelengths of both beams are calibrated by a wavelength meter with an accuracy of 0.005 nm. The final spectral resolution of PARS is about  $1.0\text{ cm}^{-1}$  in the present experiment, restricted by the linewidth of pump laser beam. The measured precision of the depolarization ratio is checked by the  $\nu_1$  ( $2917\text{ cm}^{-1}$ ) and  $\nu_3$  ( $3020\text{ cm}^{-1}$ ) vibrational modes of methane with an accuracy of 0.005.

### Liquid Raman spectroscopy

Raman spectra of liquid n-propanol and its deuterated isotopologues were recorded by a conventional spontaneous Raman experiment. The instrument and setup parameters are similar to those reported previously.<sup>[48,49]</sup> Briefly, all the experimental data were collected with a triple monochromator system (Acton Research, TriplePro) connected to a liquid-nitrogen-cooled CCD detector (Princeton Instruments, Spec-10:100B). The precision of spectral measurement with this monochromator was estimated to be better than  $0.01\text{ cm}^{-1}$  with the spectral lines of a mercury lamp, and the spectral resolution was  $\sim 1.0\text{ cm}^{-1}$ . A cw laser (Coherent, Verdi-5 W, 532 nm) was used as the light source with power output of 4 W and the laser intensity at the sample was estimated to be  $3.7 \times 10^5\text{ W/cm}^2$ . The incident laser was linearly polarized using a Glan-laser prism. The Raman scattering light was collected at  $90^\circ$  geometry relative to the incident laser beam with a pair of  $f=2.5$  and 10 cm quartz lenses, and imaged onto the entrance slit of the monochromator for spectral dispersion. The spectra were typically collected with 60 s. The Raman shifts of the spectra were calibrated with the standard lines of a mercury lamp.

### Calculations

All calculations were performed with Gaussian 09 suite of programs at DFT(B3LYP) levels of theory with standard 6-311++G(d,p) basis set,<sup>[50]</sup> including the optimized geometry, relative energy and harmonic vibrational frequency. The calculated harmonic frequencies were scaled by an empirical factor of 0.973 in both C—H bending and stretching regions to guide the assignment of experimental spectra.<sup>[27–29]</sup> To obtain the detailed interpretation of the fundamental modes of n-propanol, the potential energy distribution (PED%) is performed using freeware GAR2PED written by Martin and Alsenoy, a program to get a potential energy distribution from a Gaussian archive record.<sup>[51]</sup> The details on the frequencies, Raman activities, depolarization ratio, PED analysis and mode descriptions for five conformers of deuterated n-propanol are summarized in Table S1–3. The calculated Raman activities ( $S_i$ ) and depolarization ratios ( $\rho_i$ ) were used to evaluate Raman intensities ( $I_i$ ) of  $i$ th vibrational mode according to the Equation (1)<sup>[52]</sup>

$$I_i = \frac{f(\nu_0 - \nu_i)^4 S_i}{\nu_i(1 + \rho_i) [1 - \exp(-hc\nu_i/kT)]} \quad (1)$$

where  $\nu_0$  is the exciting wavenumber in  $\text{cm}^{-1}$ ,  $\nu_i$  is the vibrational wavenumber of  $i$ th normal mode,  $c$  is the speed of light,  $T$  is the temperature,  $h$  and  $k$  are Planck's and Boltzmann's constants, respectively, and  $f$  is a normalization factor for all peak intensities.

## Results and discussion

### Conformer analysis

The calculated geometric structures and relative energy of n-propanol are shown in Fig. 1 and summarized in Table 1. The five conformers are labeled as  $G_g$ ,  $T_g$ ,  $G'_g$ ,  $G_t$  and  $T_t$ , respectively. Capital letter refers to the CCCO orientation whereas the small letter refers to the CCOH orientation, and superscript (') indicates a negative value for the corresponding dihedral angle. Among five conformers, only  $T_t$  conformer has statistical abundance equal to 1, while the other four have statistical abundance equal to 2. This is because the  $G_t$ ,  $G'_g$ ,  $G_g$  and  $T_g$  conformers come in enantiomeric pairs and are spectroscopically and energetically undistinguishable to their mirror images  $G'_t$ ,  $G'_g$ ,  $T_g$  and  $G'_g$ , respectively.

In previous theoretical studies, the five n-propanol conformers have been placed in various energy sequences because of small energy difference.<sup>[40,42]</sup> In recent careful focal-point calculations, it was estimated that the energy difference of all five conformers was within about 0.6 kJ/mol and the  $G_t$  conformer was suggested to be the most stable form.<sup>[42]</sup> In present calculation, the  $T_t$  conformer is slightly more stable than  $G_t$  conformer by 0.04 kJ/mol when zero point energy correction is considered, as listed in Table 1. As the energy difference below 1 kJ/mol still poses a serious challenge to theory for molecule of this size, the exact energetical sequence is not pursued further in this work. Using the calculated relative energies, the populations of five conformers at room temperature (298 K) were estimated as 14:27:23:20:17 for  $T_t$ ,  $G_t$ ,  $T_g$ ,  $G_g$  and  $G'_g$  conformers, respectively. Therefore, all five conformers should be significantly populated at room temperature and contribute to the observed spectra.

### Gas-phase Raman spectra in the C—H stretching region

Figure 2 shows the polarized and depolarized Raman spectra of gaseous  $\text{CH}_3\text{CH}_2\text{CH}_2\text{OH}$ ,  $\text{CH}_3\text{CD}_2\text{CD}_2\text{OH}$ ,  $\text{CD}_3\text{CH}_2\text{CD}_2\text{OH}$  and  $\text{CD}_3\text{CD}_2\text{CH}_2\text{OH}$  in the C—H stretching region from 2700 to  $3100\text{ cm}^{-1}$  at both parallel ( $\theta=0^\circ$ ) and perpendicular ( $\theta=90^\circ$ ) polarization configurations under the same experimental conditions. To obtain peak positions and bandwidths, the spectra were fitted with Lorentz functions, as illustrated in Fig. S1 and listed in Table 2. As seen from Fig. 2, the spectra of three —CH groups overlap each other in the C—H stretching region. However, carefully comparing the observed spectra of normal and deuterated n-propanol, it is clear that every peak in normal n-propanol molecule can be well corresponded to that in deuterated molecule. Therefore, with three isotopologues, the spectral contribution from each —CH group can be clearly identified.

Compared to strong and narrow band shape in the polarized spectra, the depolarized spectra are weak and broad. To aid spectral assignment, Raman depolarization ratios of all bands observed in normal and deuterated n-propanol were measured according to  $I_{-}\theta$  curve method. The determined depolarization ratio was summarized in Table 2. When using an ideal linearly polarized excitation

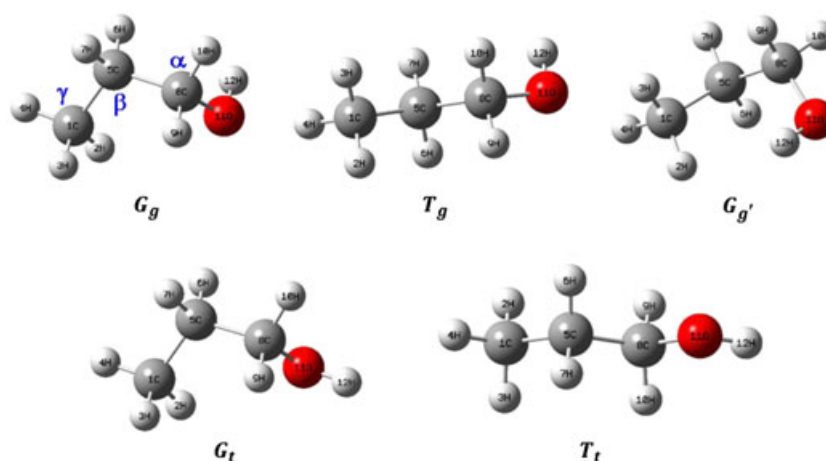


**Figure 1.** The optimized structures of five n-propanol conformers. G and g = gauche ( $60^\circ$ ), and T and t = trans ( $180^\circ$ ).

**Table 1.** Calculated relevant dihedrals and relative energy corrected by zero-point energy ( $\Delta E_{\text{ZPE}}$ ) to the five conformers of n-propanol

Conformer	CCCO ( $^\circ$ )	CCOH ( $^\circ$ )	$E_{\text{ZPE}}$ (kJ/mol)
$T_t$	180.0	180.0	0
$G_t$	63.7	-177.6	0.04
$T_g$	177.4	60.9	0.38
$G_g$	61.4	64.7	0.79
$G_g'$	65.2	-67.2	1.21

laser, the  $\rho$  value is  $0 \leq \rho < 0.75$  for a symmetric mode, whereas for an antisymmetric mode,  $\rho$  equals to 0.75. It can be seen that the values of  $\rho$  are very small and even close to zero for most bands, indicating that the bands appearing in the polarized spectra are from symmetric modes. As a matter of fact, the broad depolarized spectra are mainly contributed by antisymmetric modes although it is very weak.

### Spectral assignment of deuterated n-propanol

Using Raman intensity and the fundamental as well as possible bending overtones together with a Lorentz band shape of full widths at the half maximum (FWHM) of  $1.0 \text{ cm}^{-1}$ , the theoretical spectra of three deuterated n-propanol in the C—H stretching region were obtained and shown in Fig. 3, including the comparison with experiment. It should be noted that the positions of bending overtones are obtained by directly doubling the calculated fundamentals in order to better guide spectral assignment. The Raman intensities of overtones are arbitrary while those of the fundamentals are from the converted Raman scattering section using Equation (1). Based on depolarization ratio measurements and theoretical calculations, the Raman spectra of  $\text{CH}_3\text{CD}_2\text{CD}_2\text{OH}$ ,  $\text{CD}_3\text{CH}_2\text{CD}_2\text{OH}$ , and  $\text{CD}_3\text{CD}_2\text{CH}_2\text{OH}$  were assigned, as labeled in Fig. 3 and summarized in Table 2.

The spectrum of  $\text{CH}_3\text{CD}_2\text{CD}_2\text{OH}$  shown in Fig. 3(a) is very similar to that of  $\text{CH}_3\text{CD}_2\text{OH}$  molecule in our previous study on ethanol.<sup>[29]</sup> The strongest band at  $2948 \text{ cm}^{-1}$  was assigned to  $\text{CH}_3$  symmetric stretching ( $\text{CH}_3\text{-SS}$ ) of all five conformers, while the band at  $2890 \text{ cm}^{-1}$  and a very weak shoulder at  $2928 \text{ cm}^{-1}$  were attributed to  $\text{CH}_3$  bending overtones, which are enhanced through Fermi resonance interaction with the  $\text{CH}_3\text{-SS}$  mode. Additionally, the weak and broad band centered at  $2976 \text{ cm}^{-1}$  ( $2960\text{--}3100 \text{ cm}^{-1}$ ) was

assigned to  $\text{CH}_3$  antisymmetric stretching modes ( $\text{CH}_3\text{-AS}$ ). One can see that this band is mainly depolarized but two polarized peaks at  $2971$  and  $2980 \text{ cm}^{-1}$  lie above it, as shown in the polarized and depolarized spectrum. The depolarized component is from out-of-plane  $\text{CH}_3\text{-AS}$  and the polarized components are from in-plane  $\text{CH}_3\text{-AS}$ , where the plane denotes to the carbon-chain backbone of n-propanol ( $\text{C}_\gamma\text{-C}_\beta\text{-C}_\alpha$ ). It is known that the  $\text{CH}_3\text{-AS}$  vibration will split into two modes when local symmetry of  $\text{CH}_3$  group does not belong to  $\text{C}_{3v}$  point group, such as n-propanol molecule studied here.<sup>[28]</sup> One is out-of-plane vibration with depolarized property, and the other is in-plane one with polarized property. As shown in our recent studies, these two  $\text{CH}_3\text{-AS}$  modes are closely degenerated in frequency in most cases although their polarization properties are different.<sup>[27,28]</sup> Our measured depolarization ratio of 0.56 for  $\text{CH}_3\text{-AS}$  band support the assignment that this band is contributed by two splitting  $\text{CH}_3\text{-AS}$  modes with different polarization properties.

Compared to  $\text{CH}_3\text{-SS}$  and  $\text{CH}_3\text{-FR}$  bands, the observed  $\text{CH}_3\text{-AS}$  band is very weak. This agrees well with the general case that antisymmetric band is weak in Raman measurement whereas strong in infrared. However, the calculations predict higher intensity for  $\text{CH}_3\text{-AS}$  band, as seen from Fig. 3(a). This may be because of the limit of quantum chemistry calculation in Raman intensity. The broad feature of depolarized band originates from the fact that the antisymmetric band consists of  $\Delta J = 0, \pm 1, \pm 2$  rotational transitions, whereas the symmetric band mainly from  $\Delta J = 0$  transition in gaseous Raman measurement. Therefore, different from infrared spectrum, in which symmetric and antisymmetric stretching show similar intensities and band shape, the symmetric and antisymmetric stretching vibrations of —CH groups can be resolved in two different polarization configurations in Raman measurements. This advantage makes gas-phase Raman spectroscopy a powerful tool for resolving complex C—H spectrum. In Fig. 3(a), there is a weak band at  $2747 \text{ cm}^{-1}$ , which is from the overtone of  $\text{CH}_3$  umbrella bending according to the calculations. It may obtain the intensity through Fermi resonance with  $\text{CH}_3\text{-SS}$ .

As shown in Fig. 3(b), the spectrum of  $\text{CD}_3\text{CH}_2\text{CD}_2\text{OH}$  is very complex because of the sensitivity of  $\beta\text{-CH}_2$  stretching vibration toward conformational change of n-propanol.<sup>[33]</sup> Based on the calculations and depolarization ratio measurements, five resolvable bands at  $2952, 2942, 2932, 2926$  and  $2915 \text{ cm}^{-1}$  can be related to the  $\beta\text{-CH}_2$  symmetric stretching ( $\beta\text{-CH}_2\text{-SS}$ ) of conformers  $T_t, G_t, G_g, T_g$  and  $G_g'$ , respectively, whereas three low-frequency bands at  $2865, 2880$  and  $2890 \text{ cm}^{-1}$  can be



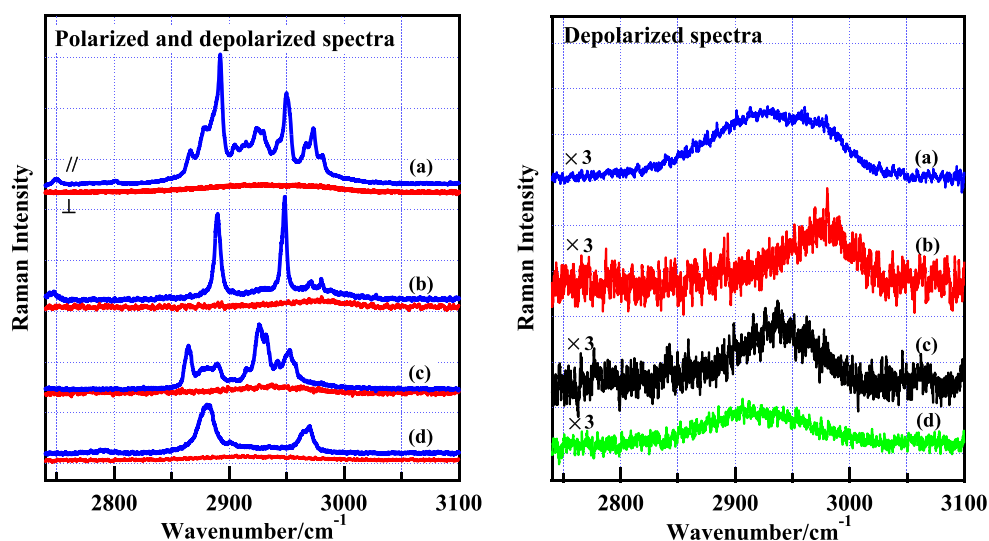


**Figure 2.** Polarized and depolarized Raman spectra of gaseous n-propanol and its deuterated isotopologues in the C—H stretching region measured under parallel (//) and perpendicular (⊥) laser polarization configurations, respectively. (a)  $\text{CH}_3\text{CH}_2\text{CH}_2\text{OH}$ ; (b)  $\text{CH}_3\text{CD}_2\text{CD}_2\text{OH}$ ; (c)  $\text{CD}_3\text{CH}_2\text{CD}_2\text{OH}$ ; (d)  $\text{CD}_3\text{CD}_2\text{CH}_2\text{OH}$ .

attributed to the Fermi resonance bands of  $\beta\text{-CH}_2$  bending overtones ( $\beta\text{-CH}_2\text{-FR}$ ).

In Fig. 3(b), the weak and broad depolarized spectrum centered at  $2939\text{ cm}^{-1}$  can be attributed to  $\beta\text{-CH}_2$  antisymmetric stretching ( $\beta\text{-CH}_2\text{-AS}$ ) vibration of five conformers, which overlaps with strong  $\beta\text{-CH}_2\text{-SS}$  mode in polarized spectrum. According to the theoretical calculation, the frequency of  $\beta\text{-CH}_2\text{-SS}$  mode is obviously lower than that of  $\beta\text{-CH}_2\text{-AS}$  mode but they are closely degenerated in the observed spectrum. This can be explained by the fact that Fermi resonance pushes the  $\beta\text{-CH}_2\text{-SS}$  fundamental to shift toward higher frequency whereas the  $\beta\text{-CH}_2\text{-AS}$  vibration is unperturbed. This reason can also be applied to explain the smaller interval between the observed  $\text{CH}_3\text{-SS}$  and  $\text{CH}_3\text{-AS}$  vibrations than the calculated one, as shown in the above spectrum of  $\text{CH}_3\text{CD}_2\text{CD}_2\text{OH}$  (Fig. 3(a)). In previous Raman study on 1,1,1,3,3,3-hexadeuteropropane ( $\text{CD}_3\text{CH}_2\text{CD}_3$ ) compound, the depolarized weak band at  $2925\text{ cm}^{-1}$  was assigned to the  $\text{CH}_2$  antisymmetric stretching.<sup>[53]</sup> As the  $\text{-CH}_2$  groups in  $\text{CD}_3\text{CH}_2\text{CD}_2\text{OH}$  and  $\text{CD}_3\text{CH}_2\text{CD}_3$  have similar surroundings, their spectral characteristics should be similar. Although the observed  $\beta\text{-CH}_2\text{-AS}$  mode is weak in our gaseous Raman spectrum, it may show relatively large intensity in IR or SFG measurements. This is because SFG response is the product of the IR transition dipole and Raman polarizabilities.

For the spectrum of  $\text{CD}_3\text{CD}_2\text{CH}_2\text{OH}$  shown in Fig. 3(c), the strong band at  $2880\text{ cm}^{-1}$  was assigned to the  $\alpha\text{-CH}_2$  symmetric stretching ( $\alpha\text{-CH}_2\text{-SS}$ ) whereas another band at  $2968\text{ cm}^{-1}$  belongs to Fermi resonance mode of bending overtones ( $\alpha\text{-CH}_2\text{-FR}$ ). The weak band at  $2790\text{ cm}^{-1}$  is from the  $\alpha\text{-CH}_2$  rocking overtone according to the calculations. It should be mentioned that there is a weak shoulder at  $2901\text{ cm}^{-1}$  unassigned. Contrasted to theoretical calculation, this polarized band is mostly possible from the  $\alpha\text{-CH}_2\text{-SS}$  of the  $G_9$  conformer although it is also possible from the Fermi resonance of  $\alpha\text{-CH}_2$  bending overtone of the  $G_9$  conformer. However, if the latter case is true, the frequency of Fermi resonance band is too close to  $\alpha\text{-CH}_2\text{-SS}$  fundamental. The depolarized spectrum centered at  $2931\text{ cm}^{-1}$  was assigned to the antisymmetric stretching of  $\alpha\text{-CH}_2$  group ( $\alpha\text{-CH}_2\text{-AS}$ ), as labeled in Fig. 3(c). The spectral feature of  $\text{CD}_3\text{CD}_2\text{CH}_2\text{OH}$  molecule is very similar to deuterated ethanol  $\text{CD}_3\text{CH}_2\text{OH}$ , including the weak and broad  $\text{CH}_2\text{-AS}$  band.<sup>[29]</sup>

Comparing the depolarized spectra of three deuterated n-propanol, one can find that the band shape of  $\alpha\text{-CH}_2\text{-AS}$  is much broader than those of  $\beta\text{-CH}_2\text{-AS}$  and  $\text{CH}_3\text{-AS}$ . This is in good agreement with the theoretical calculation that the  $\alpha\text{-CH}_2\text{-AS}$  mode exhibits the larger frequency variability among five conformers than that of  $\beta\text{-CH}_2\text{-AS}$  and  $\text{CH}_3\text{-AS}$  modes. As listed in Table S1–3, the frequency variability of the  $\alpha\text{-CH}_2\text{-AS}$  mode is  $80\text{ cm}^{-1}$  among five conformers of  $\text{CD}_3\text{CD}_2\text{CH}_2\text{OH}$  molecule whereas that of  $\beta\text{-CH}_2\text{-AS}$  mode and  $\text{CH}_3\text{-AS}$  mode is  $31\text{ cm}^{-1}$  and  $32\text{ cm}^{-1}$ , respectively.

From above assignment, it can be seen that Fermi resonance interaction and different molecular conformations play an important role in determining band shape of n-propanol in the C—H stretching region. However, it is still a challenge to accurately reproduce these Fermi resonance pairs from a theoretical view. In this study, although the theoretical spectra do not agree well with experimental one, including relative frequency shift and Raman intensity, it provides reasonable support for the assignment of experimental spectra, especially when considering that Fermi resonance pushes the high-frequency mode to shift toward higher energy whereas the low-frequency mode to shift toward lower energy. The further theoretical works based on anharmonic models are needed to accurately predict the spectral details in the C—H stretching region, especially the influence of Fermi resonance.

### Comparison of $\text{CH}_3$ and $\text{CH}_2$ stretching vibrations

From theoretical and experimental spectra of all three deuterated n-propanol, it can be seen that the C—H stretching vibration at different sites of carbon backbone chain exhibits different sensitivity to conformational changes of n-propanol molecule. Obviously, the  $\text{CH}_2$  stretching vibrations at both  $\alpha$ -carbon and  $\beta$ -carbon atoms are sensitive whereas the  $\text{CH}_3$  stretching vibration at terminated  $\gamma$ -carbon is not sensitive, leading to narrower band shape in the spectrum of  $\text{CH}_3\text{CD}_2\text{CD}_2\text{OH}$  molecule compared with  $\text{CD}_3\text{CH}_2\text{CD}_2\text{OH}$  and  $\text{CD}_3\text{CD}_2\text{CH}_2\text{OH}$  molecules, as seen from Fig. 3. For  $\text{CH}_2$  group, the symmetric stretching mode at  $\beta$ -carbon atom is more sensitive to conformational change than that of  $\alpha$ -carbon atom and can be used as a new probe to identify all five conformers. However, for

**Table 2.** Observed Raman band position ( $\text{cm}^{-1}$ ), width ( $\text{cm}^{-1}$ ) and depolarization ratios of deuterated and normal n-propanol in the gaseous and liquid phases, as well as their assignments in the C—H stretching region

Molecules	Gas phase			Liquid phase		$\Delta^b$	Spectral assignments			
	Position	Width <sup>a</sup>	$\rho$	Position	Width		This work	Ref 35	Ref 16	Ref 34
$\text{CH}_3\text{CD}_2\text{CD}_2\text{OH}$	2747	9.8	0.09				CH <sub>3</sub> umbrella overtone			
	2890	5.9	0.023	2876	11.2	−14	CH <sub>3</sub> -FR			
	2928	31.2	0.301	2917	45.0	−11	CH <sub>3</sub> -FR			
	2948	4.6	0.053	2935	10.8	−13	CH <sub>3</sub> -SS			
	2976	30.2	0.569	2967	27.0	−9	CH <sub>3</sub> -AS			
	2976 (depolarized)	62.2					CH <sub>3</sub> -AS			
$\text{CD}_3\text{CH}_2\text{CD}_2\text{OH}$	2865	6.0	0.060	2854	11.9	−11	$\beta$ -CH <sub>2</sub> -FR			
	2878	11.7	0.100				$\beta$ -CH <sub>2</sub> -FR			
	2890	10.8	0.089	2873	14.1	−17	$\beta$ -CH <sub>2</sub> -FR			
	2915	6.0	0.290				$\beta$ -CH <sub>2</sub> -SS			
	2926	8.1	0.108	2917 <sup>c</sup>	19.5	−9	$\beta$ -CH <sub>2</sub> -SS			
	2932	5.4	0.113				$\beta$ -CH <sub>2</sub> -SS			
	2942	2.8	0.210				$\beta$ -CH <sub>2</sub> -SS			
2952	14.8	0.096	2941 <sup>c</sup>	16.3	−11	$\beta$ -CH <sub>2</sub> -SS				
2939 (depolarized)	75.3					$\beta$ -CH <sub>2</sub> -AS				
$\text{CD}_3\text{CD}_2\text{CH}_2\text{OH}$	2790	16.0	0.05				$\alpha$ -CH <sub>2</sub> rocking overtone			
	2880	15.7	0.064	2873	41.4	−7	$\alpha$ -CH <sub>2</sub> -SS			
	2900		0.289				$\alpha$ -CH <sub>2</sub> -SS			
	2931	58		2925	40	−6	$\alpha$ -CH <sub>2</sub> -AS			
	2968	12.1	0.140	2952	24.3	−16	$\alpha$ -CH <sub>2</sub> -FR			
2931 (depolarized)	116.0					$\alpha$ -CH <sub>2</sub> -AS				
$\text{CH}_3\text{CH}_2\text{CH}_2\text{OH}$	2750		0.05				CH <sub>3</sub> umbrella overtone			
	2866		0.098	2852		−14	$\beta$ -CH <sub>2</sub> -FR			
	2879		0.077				$\alpha$ -CH <sub>2</sub> -SS and $\beta$ -CH <sub>2</sub> -FR			
	2892		0.059	2876 <sup>d</sup>		−16	CH <sub>3</sub> -FR and $\beta$ -CH <sub>2</sub> -FR			
	2905		0.124				$\alpha$ -CH <sub>2</sub> -SS			
	2915		0.133				$\beta$ -CH <sub>2</sub> -SS			
	2923		0.109	2911 <sup>c</sup>		−12	$\beta$ -CH <sub>2</sub> -SS			
	2928		0.115				$\beta$ -CH <sub>2</sub> -SS			
	2942		0.137				$\beta$ -CH <sub>2</sub> -SS			
	2950		0.116	2936		−14	CH <sub>3</sub> -SS and $\beta$ -CH <sub>2</sub> -SS			
	2966		0.197				CH <sub>3</sub> -AS			
	2973		0.098	2960		−13	$\alpha$ -CH <sub>2</sub> -FR and CH <sub>3</sub> -AS			
2981		0.077				CH <sub>3</sub> -AS				

<sup>a</sup>Full width at half maximum.<sup>b</sup>The difference of band position between the liquid and gas phase.<sup>c</sup>This band includes a little contribution from  $\beta$ -CH<sub>2</sub>-AS.<sup>d</sup>This band should be assigned as the overlapping between CH<sub>3</sub>-FR,  $\beta$ -CH<sub>2</sub>-FR and  $\alpha$ -CH<sub>2</sub>-SS modes in liquid n-propanol.

antisymmetric stretching vibration, the CH<sub>2</sub> group at  $\alpha$ -carbon atom is more sensitive than that of  $\beta$ -carbon atom. As a result, the depolarized spectrum of CD<sub>3</sub>CD<sub>2</sub>CH<sub>2</sub>OH molecule is significantly broadened compared with CD<sub>3</sub>CD<sub>2</sub>CH<sub>2</sub>OH molecule and CH<sub>3</sub>CD<sub>2</sub>CD<sub>2</sub>OH, as mentioned early. In recent theoretical studies, Šebek *et al.* investigated C—H stretching Raman spectra on a serial of selected organic molecules using vibrational self-consistent field method.<sup>[20]</sup> One important conclusion is that the frequencies of CH<sub>3</sub> stretching vibrations do not significantly depend on the surroundings of the functional group and so the absorption bands of CH<sub>3</sub> group can always be expected at similar position. However, unlike CH<sub>3</sub> group, the symmetric and antisymmetric stretching vibrations of CH<sub>2</sub> group are highly dependent on the neighboring groups and geometric structures of molecules. This conclusion is consistent with the spectral behaviors of CH<sub>3</sub> and CH<sub>2</sub> groups in n-propanol molecule presented here.

### Spectral assignment of normal n-propanol

With the spectra of three deuterated n-propanol assigned, it is easy to make an unambiguous assignment for Raman spectra of normal n-propanol in the C—H stretching region, as summarized in Table 2, along with those results from other experimental techniques. It can be seen that there are many overlapping spectral features among three —CH groups, which were not found previously. In recent studies, based on the polarization selection rules of methyl and methylene groups at air/liquid interface, the overlapping spectral features between the CH<sub>3</sub> and CH<sub>2</sub> groups were identified for short-chain ethanol molecule (CH<sub>3</sub>CH<sub>2</sub>OH) using SFG spectroscopy.<sup>[15]</sup> The results show that the methylene Fermi resonance mode, which appears in the region of 2960–2970  $\text{cm}^{-1}$ , overlaps with the methyl antisymmetric stretching mode at about 2970  $\text{cm}^{-1}$ , but they can be distinguished in different polarization

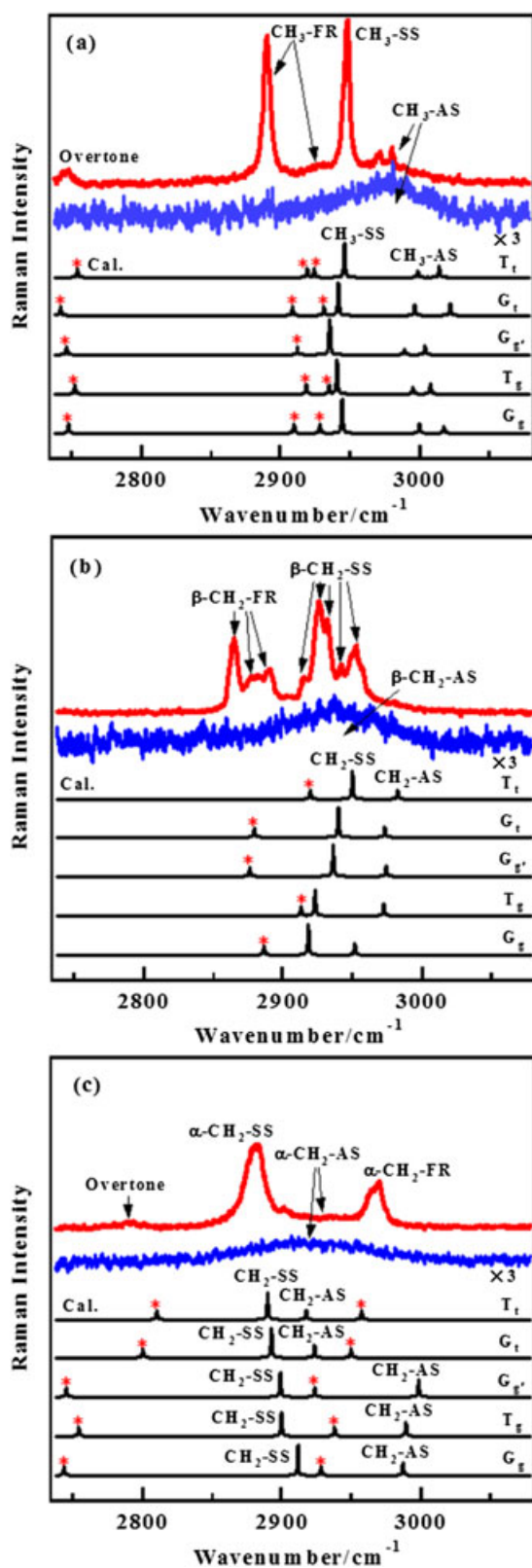


**Figure 3.** The calculated Raman spectra for five conformers of three deuterated n-propanol in the C—H stretching region along with experimental spectra. For the visual clarity, the depolarized spectra were enlarged by three times. The red star (\*) denotes the calculated  $\text{CH}_2$  or  $\text{CH}_3$  bending overtones whose intensities are arbitrary, and their frequencies are obtained by directly doubling the calculated bending fundamentals. SS, symmetric stretching; AS, antisymmetric stretching; FR, Fermi resonance. (a)  $\text{CH}_3\text{CD}_2\text{CD}_2\text{OH}$ ; (b)  $\text{CD}_3\text{CH}_2\text{CD}_2\text{OH}$ ; (c)  $\text{CD}_3\text{CD}_2\text{CH}_2\text{OH}$ .

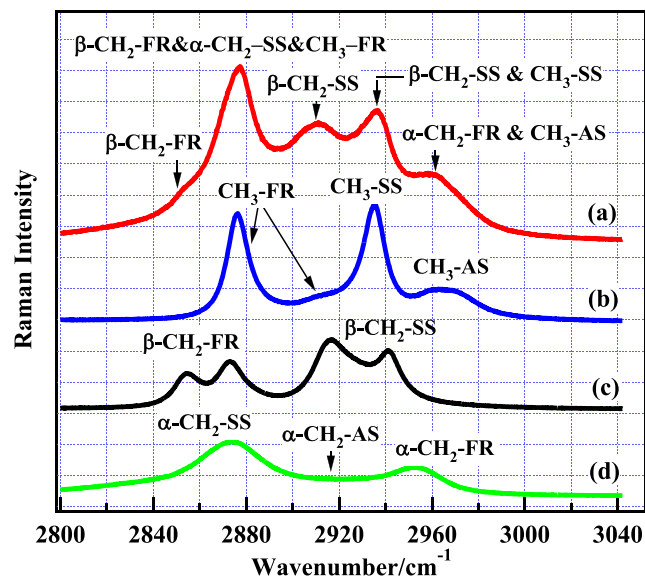


**Figure 4.** Liquid Raman spectra of n-propanol and three deuterated isotopologues in the C—H stretching region. (a)  $\text{CH}_3\text{CH}_2\text{CH}_2\text{OH}$ ; (b)  $\text{CH}_3\text{CD}_2\text{CD}_2\text{OH}$ ; (c)  $\text{CD}_3\text{CH}_2\text{CD}_2\text{OH}$ ; (d)  $\text{CD}_3\text{CD}_2\text{CH}_2\text{OH}$ .

combinations of incident laser beams. This result is consistent with that in this work that the band of normal n-propanol at  $2973\text{ cm}^{-1}$  is overlapped by antisymmetric stretching mode of methyl group and Fermi resonance peak of methylene group at  $\alpha$ -carbon atom, as shown in Fig. 2 and Table 2. The overlapping of methyl antisymmetric stretching mode and  $\alpha$ -carbon methylene Fermi resonance mode at  $\sim 2970\text{ cm}^{-1}$  should be a common spectral feature in the straight-chain 1-alcohols.

### Liquid Raman spectroscopy

The C—H stretching Raman spectra of liquid normal and deuterated n-propanol were presented in Fig. 4. To obtain peak positions and bandwidths, the spectra were fitted with Lorentz functions, as listed in Table 2 and shown in Fig. S1. It can be seen that spectral features in liquid state are very similar to those in gas phase except for the band broadening and red shifts of peak positions. Because spectral resolution in present experiment is about  $1.0\text{ cm}^{-1}$ , the main origin of band broadening should be from molecular interactions in liquid n-propanol, such as hydrogen (H)-bond effect. It is known that liquid n-propanol molecules form O—H...O H-bond cluster with ring or chain structures, which can significantly broaden the vibrational bands, especially in the O—H stretching region. As a consequence, many spectral details that are observed in the gas phase become obscured in liquid state. For example, the bands of  $\beta$ - $\text{CH}_2$  symmetric stretching corresponding to five gas-phase conformers are no longer well resolved in liquid spectra of  $\text{CD}_3\text{CH}_2\text{CD}_2\text{OH}$  and  $\text{CH}_3\text{CH}_2\text{CH}_2\text{OH}$ . In addition, the shoulder at  $2901\text{ cm}^{-1}$  from  $\alpha$ - $\text{CH}_2$ -SS of the  $G_9$  conformer in gaseous  $\text{CD}_3\text{CD}_2\text{CH}_2\text{OH}$  and  $\text{CH}_3\text{CH}_2\text{CH}_2\text{OH}$  disappears in the corresponding liquid spectra. Therefore, compared to liquid state, the gas-phase Raman spectroscopy can capture more spectral details, which are necessary for accurate assignments. Based on the gas-phase analysis, the liquid spectra are reassigned.

Although most bands are obviously broadened in liquid state, the bands from antisymmetric stretching modes become narrow and strong in liquid state. For example, in gaseous  $\text{CH}_3\text{CD}_2\text{CD}_2\text{OH}$  molecule, the bandwidth (FWHM) of  $\text{CH}_3$ -AS is  $30\text{ cm}^{-1}$  whereas it

is changed to  $27\text{ cm}^{-1}$  in liquid state, as shown in Table 2. As mentioned early, the symmetric band mainly consists of Q-branch ( $\Delta J=0$  transition) in Raman measurement, whereas the antisymmetric band consists of  $\Delta J=0, \pm 1, \pm 2$  rotational transitions, leading to broad and diffuse spectral contour in the gas phase. However, the molecular rotation can be effectively quenched by the intermolecular interaction in liquid state. As a result, the antisymmetric stretching band becomes relatively narrow and strong compared to gas phase although it is also broadened by intermolecular interactions in liquid state.

The overall red-shifts of C—H stretching bands can be attributed to the solvation interaction effect in liquid n-propanol, such as dielectric contribution, dipolar interaction and basicity or acidity.<sup>[54]</sup> Further comparisons show that the red shifts of the  $C_{\alpha}H_2$ -SS and  $C_{\alpha}H_2$ -AS modes of  $CD_3CD_2CH_2OH$  molecule are the smallest among all the bands. This may be because of the fact that  $\alpha$ - $CH_2$  group is directly connected to —OH group which forms strong O—H...O H-bond in liquid n-propanol. As revealed in recent experimental and theoretical studies, the O—H...O H-bond interaction can cause the blue shift of C—H stretching band in pure alcohols or in alcohol–water mixtures.<sup>[54–56]</sup> That is to say, the blue shift is an indirect effect from the interaction of adjacent functional groups with solvent molecules. In further study on the long-chain 2-butoxyethanol ( $C_4E_1$ )/water system, it is shown that the frequency of  $CH_2$  groups directly connected to the ether oxygen atom, which interacts with the water molecules through H-bond networks, exhibits a more significant blue shift, whereas the other  $CH_3$  or  $CH_2$  groups do not. Therefore, besides red shift, the C—H bands blue shift because of the H-bond interaction and the largest blue shift occurs for the  $\alpha$ - $CH_2$  group of liquid n-propanol. The red-shifts and blue-shifts act in opposite directions, and the resulting frequency is a balance of these two effects. In addition to the smallest red-shift, the band broadening of  $\alpha$ - $CH_2$  group is the most obvious among all bands. From Table 2, it can be seen that the bandwidth (FWHM) of  $C_{\alpha}H_2$ -SS mode changes from  $16\text{ cm}^{-1}$  to  $41\text{ cm}^{-1}$  in the spectra of  $CD_3CD_2CH_2OH$  molecule on going from the gas phase to liquid phase. This may also indirectly caused by H-bond interactions, which have more impact on the adjacent  $\alpha$ - $CH_2$  group.

## Conclusion

In this study, Raman spectra of three deuterated and normal n-propanol have been investigated in both gas phase and liquid phase with stimulated PARS and conventional spontaneous Raman spectroscopy, respectively. Isotope substitution allowed unequivocal identification of the spectral contribution of each C—H groups in n-propanol molecules. Assignments of observed gas-phase Raman spectra were facilitated by depolarization ratio measurement and quantum chemical calculations carried out at DFT (B3LYP) level of theory. It is found that vibrational spectra of n-propanol in the C—H stretching region are far more complex than previously determined, and exhibits many overlapping spectral features among three —CH groups because of Fermi resonance interaction and different molecular conformations. The new assignments in both gaseous and liquid n-propanol clarified the confusions in previous studies and provided a reliable groundwork for the spectral application in the futures. The further comparisons between the gas-phase spectra of three deuterated n-propanol reveal that the  $CH_3$  stretching vibrations are not significantly sensitive to the neighboring groups and geometric structures of molecules whereas those of  $CH_2$  groups are highly dependent. These results are of great

importance when considering that hydrocarbon chains are structures unit in organic and biological molecules. In addition, the molecular interactions in liquid n-propanol are analyzed based on the spectral changes of observed C—H bands in gas and liquid phases.

## Acknowledgements

The present work was supported financially by the National Natural Science Foundation of China (NSFC, 20903002, 21273211, 21573208) and Anhui Provincial Natural Science Foundation (1408085MA18), Anhui Provincial Educational Ministry (KJ2015A040) and National Key Basic Research Special Foundation (NKBRFSF, 2013CB834602).

## References

- [1] C. J. Gruenloh, G. M. Florio, J. R. Carney, F. C. Hagemester, T. S. Zwier, *J. Phys. Chem. A* **1999**, *103*, 496.
- [2] S. Jarmelo, N. Maiti, V. Anderson, P. R. Carey, R. Fausto, *J. Phys. Chem. A* **2005**, *109*, 2069.
- [3] A. A. Liu, S. Liu, R. D. Zhang, Z. F. Ren, *J. Phys. Chem. C* **2015**, *119*, 23486.
- [4] L. Chen, W. D. Zhu, K. Lin, N. Y. Hu, Y. Q. Yu, X. G. Zhou, L. F. Yuan, S. M. Hu, Y. Luo, *J. Phys. Chem. A* **2015**, *119*, 3209.
- [5] E. G. Buchanan, E. L. Sibert, T. S. Zwier, *J. Phys. Chem. A* **2013**, *117*, 2800.
- [6] Z. H. Wang, A. Pakoulev, D. D. Dlott, *Science* **2002**, *296*, 2201.
- [7] C. L. Evans, E. O. Potma, M. Puoris'haag, D. Cote, C. P. Lin, X. S. Xie, *Proc. Natl. Acad. Sci. U. S. A.* **2005**, *102*, 16807.
- [8] C. W. Freudiger, W. Min, B. G. Saar, S. Lu, G. R. Holtom, C. W. He, J. C. Tsai, J. X. Kang, X. S. Xie, *Science* **2008**, *322*, 1857.
- [9] P. S. Walsh, J. C. Dean, C. McBurney, H. Kang, S. H. Gellman, T. S. Zwier, *Phys. Chem. Chem. Phys.* **2016**, *18*, 11306.
- [10] H. J. Tong, J. Y. Yu, Y. H. Zhang, J. P. Reid, *J. Phys. Chem. A* **2010**, *114*, 6795.
- [11] T. N. Wassermann, P. Zielke, J. J. Lee, C. Cezard, M. A. Suhm, *J. Phys. Chem. A* **2007**, *111*, 7437.
- [12] R. A. Macphail, H. L. Strauss, R. G. Snyder, C. A. Elliger, *J. Phys. Chem.* **1984**, *88*, 334.
- [13] R. G. Snyder, H. L. Strauss, C. A. Elliger, *J. Phys. Chem.* **1982**, *86*, 5145.
- [14] R. G. Snyder, J. R. Scherer, *J. Chem. Phys.* **1979**, *71*, 3221.
- [15] W. Gan, Z. Zhang, R. R. Feng, H. F. Wang, *Chem. Phys. Lett.* **2006**, *423*, 261.
- [16] R. Lu, W. Gan, B. H. Wu, Z. Zhang, Y. Guo, H. F. Wang, *J. Phys. Chem. B* **2005**, *109*, 14118.
- [17] R. Lu, W. Gan, B. H. Wu, H. Chen, H. F. Wang, *J. Phys. Chem. B* **2004**, *108*, 7297.
- [18] H. F. Wang, W. Gan, R. Lu, Y. Rao, B. H. Wu, *Int. Rev. Phys. Chem.* **2005**, *24*, 191.
- [19] S. A. Fischer, T. W. Ueltschi, P. Z. El-Khoury, A. L. Mifflin, W. P. Hess, H. F. Wang, C. J. Cramer, N. Govind, *J. Phys. Chem. B* **2016**, *120*, 1429.
- [20] J. Sebek, R. Knaanie, B. Albee, E. O. Potma, R. B. Gerber, *J. Phys. Chem. A* **2013**, *117*, 7442.
- [21] J. Sebek, L. Pele, E. O. Potma, R. B. Gerber, *Phys. Chem. Chem. Phys.* **2011**, *13*, 12724.
- [22] L. Pele, J. Sebek, E. O. Potma, R. B. Gerber, *Chem. Phys. Lett.* **2011**, *515*, 7.
- [23] E. L. Sibert, D. P. Tabor, N. M. Kidwell, J. C. Dean, T. S. Zwier, *J. Phys. Chem. A* **2014**, *118*, 11272.
- [24] E. L. Sibert, N. M. Kidwell, T. S. Zwier, *J. Phys. Chem. B* **2014**, *118*, 8236.
- [25] E. L. Sibert, *Mol. Phys.* **2013**, *111*, 2093.
- [26] E. G. Buchanan, J. C. Dean, T. S. Zwier, E. L. Sibert, *J. Chem. Phys.* **2013**, *138*, 064308.
- [27] Y. Q. Yu, Y. X. Wang, N. Y. Hu, K. Lin, X. G. Zhou, S. L. Liu, *J. Raman Spectrosc.* **2014**, *45*, 259.
- [28] Y. Q. Yu, Y. X. Wang, K. Lin, N. Y. Hu, X. G. Zhou, S. L. Liu, *J. Phys. Chem. A* **2013**, *117*, 4377.
- [29] Y. Q. Yu, K. Lin, X. G. Zhou, H. Wang, S. L. Liu, X. X. Ma, *J. Phys. Chem. C* **2007**, *111*, 8971.
- [30] S. Kataoka, P. S. Cremer, *J. Am. Chem. Soc.* **2006**, *128*, 5516.
- [31] J. H. Sung, K. Park, D. Kim, *J. Phys. Chem. B* **2005**, *109*, 18507.
- [32] L. K. Iwaki, D. D. Dlott, *J. Phys. Chem. A* **2000**, *104*, 9101.
- [33] Y. Q. Yu, Y. X. Wang, N. Y. Hu, K. Lin, X. G. Zhou, S. L. Liu, *Phys. Chem. Chem. Phys.* **2016**, *18*, 10563.



- [34] N. Michniewicz, A. S. Muszynski, W. Wrzeszcz, M. A. Czarnecki, B. Golec, J. P. Hawranek, Z. Mielke, *J. Mol. Struct.* **2008**, *887*, 180.
- [35] H. G. M. Edwards, D. W. Farwell, R. D. Bowen, *J. Mol. Struct.* **2007**, *832*, 184.
- [36] V. Barone, *J. Chem. Phys.* **2005**, 122.
- [37] V. Barone, G. Festa, A. Grandi, N. Rega, N. Sanna, *Chem. Phys.Lett.* **2004**, *388*, 279.
- [38] V. Barone, *J. Phys. Chem. A* **2004**, *108*, 4146.
- [39] T. N. Wassermann, M. A. Suhm, P. Roubin, S. Coussan, *J. Mol. Struct.* **2012**, *1025*, 20.
- [40] Z. Kisiel, O. Dorosh, A. Maeda, I. R. Medvedev, F. C. De Lucia, E. Herbst, B. J. Drouin, J. C. Pearson, S. T. Shipman, *Phys. Chem. Chem. Phys.* **2010**, *12*, 8329.
- [41] Z. H. Luo, C. G. Ning, K. Liu, Y. R. Huang, J. K. Deng, *J Phys. B-At. Mol. Opt.* **2009**, 42.
- [42] K. Kahn, T. C. Bruice, *Chemphyschem* **2005**, *6*, 487.
- [43] N. G. Mirkin, S. Krimm, *Biopolymers* **2009**, *91*, 791.
- [44] C. S. Miller, E. A. Ploetz, M. E. Cremeens, S. A. Corcelli, *J. Chem. Phys.* **2009**, *130*, 125103.
- [45] N. G. Mirkin, S. Krimm, *J. Phys. Chem. A* **2007**, *111*, 5300.
- [46] M. Epshtein, A. Portnov, N. Mayorkas, S. Rosenwaks, B. Brauer, I. Bar, *J. Phys. Chem. A* **2013**, *117*, 11618.
- [47] Y. Q. Yu, K. Lin, X. G. Zhou, H. Wang, S. L. Liu, X. X. Ma, *J. Raman Spectrosc.* **2007**, *38*, 1206.
- [48] K. Lin, N. Y. Hu, X. G. Zhou, S. L. Liu, Y. Luo, *J. Raman Spectrosc.* **2012**, *43*, 82.
- [49] K. Lin, X. G. Zhou, Y. Luo, S. L. Liu, *J. Phys. Chem. B* **2010**, *114*, 3567.
- [50] M. J. Frisch, G. W. Trucks, H. B. Schlegel, G. E. Scuseria, M. A. Robb, J. R. Cheeseman, G. Scalmani, V. Barone, B. Mennucci, G. A. Petersson, et al., GAUSSIAN 09 (Reversion B.01), Gaussian, Inc., Pittsburgh **2009**.
- [51] J. M. L. Martin, C. V. Alsenoy, GAR2PED, University of Antwerp, Belgium **1995**.
- [52] N. Mayorkas, A. Bernat, S. Izbitski, I. Bar, *J. Chem. Phys.* **2013**, *138*, 124312.
- [53] G. Zerbi, S. Abbate, *Chem. Phys.Lett.* **1981**, *80*, 455.
- [54] Y. Katsumoto, H. Komatsu, K. Ohno, *J. Am. Chem. Soc.* **2006**, *128*, 9278.
- [55] T. Shimoaka, Y. Katsumoto, *J. Phys. Chem. A* **2010**, *114*, 11971.
- [56] C. D. Keefe, E. A. L. Gillis, L. MacDonald, *J. Phys. Chem. A* **2009**, *113*, 2544.

## Supporting information

Additional supporting information may be found in the online version of this article at the publisher's web site.